

# Astrometry with digital sky surveys: from SDSS to LSST

Ž. Ivezić<sup>1</sup>, D. G. Monet<sup>2</sup>, N. Bond<sup>3</sup>, M. Jurić<sup>4</sup>, B. Sesar<sup>1</sup>, J. A. Munn<sup>2</sup>, R. H. Lupton<sup>3</sup>, J. E. Gunn<sup>3</sup>, G. R. Knapp<sup>3</sup>, A. J. Tyson<sup>5</sup>, P. Pinto<sup>6</sup>, K. Cook<sup>7,8</sup>, SDSS Collaboration and LSST Collaboration

<sup>1</sup>Department of Astronomy, University of Washington, Box 351580, Seattle, WA 98195  
email: ivezic@astro.washington.edu

<sup>2</sup>U.S. Naval Observatory, Flagstaff Station, P.O. Box 1149, Flagstaff, AZ 86002 <sup>3</sup>Princeton University Observatory, Princeton, NJ 08544 <sup>4</sup>Institute for Advanced Study, 1 Einstein Drive, Princeton, NJ 08540 <sup>5</sup>Physics Department, University of California, One Shields Avenue, Davis, CA 95616 <sup>6</sup>Steward Observatory, University of Arizona, 933 N Cherry Ave., Tucson, AZ 85721 <sup>7</sup>Lawrence Livermore National Laboratory, 7000 East Avenue, Livermore, CA 94550 <sup>8</sup>KHC's work was performed under the auspices of the U.S. D.O.E. by LLNL under contract DE-AC52-07NA27344

**Abstract.** Major advances in our understanding of the Universe have historically come from dramatic improvements in our ability to accurately measure astronomical quantities. The astrometric observations obtained by modern digital sky surveys are enabling unprecedentedly massive and robust studies of the kinematics of the Milky Way. For example, the astrometric data from the Sloan Digital Sky Survey (SDSS), together with half a century old astrometry from the Palomar Observatory Sky Survey (POSS), have enabled the construction of a catalog that includes absolute proper motions as accurate as 3 mas/year for about 20 million stars brighter than  $V=20$ , and for 80,000 spectroscopically confirmed quasars which provide exquisite error assessment. We discuss here several ongoing studies of Milky Way kinematics based on this catalog. The upcoming next-generation surveys will maintain this revolutionary progress. For example, we show using realistic simulations that the Large Synoptic Survey Telescope (LSST) will measure proper motions accurate to 1 mas/year to a limit 4 magnitude fainter than possible with SDSS and POSS catalogs, or with the Gaia survey. LSST will also obtain geometric parallaxes with accuracy similar to Gaia's at its faint end (0.3 mas at  $V=20$ ), and extend them to  $V=24$  with an accuracy of 3 mas. We discuss the impact that these LSST measurements will have on studies of the Milky Way kinematics, and potential synergies with the Gaia survey.

**Keywords.** astrometry, catalogs, surveys

---

## 1. Introduction

The astrometric observations obtained by modern massive digital sky surveys, such as SDSS, 2MASS, and FIRST, are enabling numerous unprecedented studies extending from solar system to extragalactic astronomy. In this contribution we describe several results on the kinematics of Milky Way stars based on proper motions obtained by comparing POSS and SDSS astrometric measurements. The main advantages of this data set are the large sample size and distance limits, as well as excellent photometry that enables accurate metallicity estimates for F/G main sequence stars. All these data characteristics will be significantly enhanced by LSST thanks to its 2 magnitude fainter imaging limit, and close to a thousand observations in six bandpasses over about half of the sky.

## 2. The analysis of the Milky Way stellar kinematics based on SDSS

### 2.1. An overview of the Sloan Digital Sky Survey

The SDSS is a digital photometric and spectroscopic survey which will cover about one quarter of the Celestial Sphere in the North Galactic cap, and produce a smaller area ( $\sim 300 \text{ deg}^2$ ) but much deeper survey in the Southern Galactic hemisphere (Adelman-McCarthy *et al.* 2006, and references therein). SDSS provides deep ( $r < 22.5$ ) photometry in five *ugriz* bandpasses with errors of order 0.02 mag for sources not limited by photon statistics. The recent Data Release 6 catalogs 287 million unique objects detected in  $9583 \text{ deg}^2$  of sky. A compendium of technical details about SDSS can be found on the SDSS web site (<http://www.sdss.org>), which also provides the interface for public data access.

The SDSS astrometric reductions are described in detail by Pier *et al.* (2003). Briefly, SDSS absolute astrometric accuracy is better than 100 mas, with relative (band-to-band) accuracy of about 20–30 mas (rms, for sources not limited by photon statistics). In addition to providing positions for a large number of objects with remarkable accuracy (and thus enabling recalibration of other less accurate surveys, as described below), an important characteristic of SDSS astrometric observations is that measurements in five photometric bands are obtained over a five minute long period (with 54 sec per exposure). The multi-color nature allows the discovery of the so-called Color Induced Displacement binary stars (for details see Pourbaix *et al.* 2004), and the time delay allows the recognition of asteroids (Ivezić *et al.* 2001). Here we focus on studies of stellar proper motions enabled by SDSS astrometric measurements.

### 2.2. Proper motions determined from SDSS and POSS astrometric observations

We use proper motion measurements from the Munn *et al.* (2004) catalog, which is based on astrometric measurements from SDSS and a collection of Schmidt photographic surveys. Despite the sizable random and systematic astrometric errors in the Schmidt surveys, the combination of a long baseline ( $\sim 50$  years for POSS-I survey), and a recalibration of the photographic data using positions of SDSS galaxies, results in median random errors for proper motions of only  $\sim 3 \text{ mas/year}$  for  $g < 19.5$  (per component). Systematic errors are typically an order of magnitude smaller, as robustly determined using  $\sim 80,000$  spectroscopically confirmed SDSS quasars from Schneider *et al.* (2007). At a distance of 1 kpc, a random error of 3 mas/year corresponds to a velocity error of  $\sim 15 \text{ km/s}$ , which is comparable to the radial velocity accuracy delivered by the SDSS stellar spectroscopic survey.

The kinematics of the SDSS stellar sample, including mutual consistency of kinematics based on radial velocity and proper motion measurements, are discussed in detail by Bond *et al.* (2008, in prep.). Here we briefly present a few results that are directly related to the conclusions of this paper.

### 2.3. Analysis of SDSS-POSS proper motion database

Most available studies of stellar motions are confined to the solar neighborhood. For example, Hipparcos has enabled detailed mapping of velocity distribution for  $\sim 12,000$  stars within  $\sim 100 \text{ pc}$  (Dehnen & Binney 1998). With the SDSS-POSS proper motion measurements, analogous analysis can be extended to a distance limit of 10 kpc, with a sample including close to 20 million main-sequence stars.

In this contribution we limit our analysis to  $\sim 330,000$  stars observed towards the north galactic pole ( $b > 80^\circ$ ), with  $14.5 < r < 20$ , and colors consistent with main-sequence stars (Jurić *et al.* 2008). We further split this sample into three subsamples, as follows. The main-sequence stars with F/G spectral types, selected by  $0.2 < g - r < 0.4$ , are

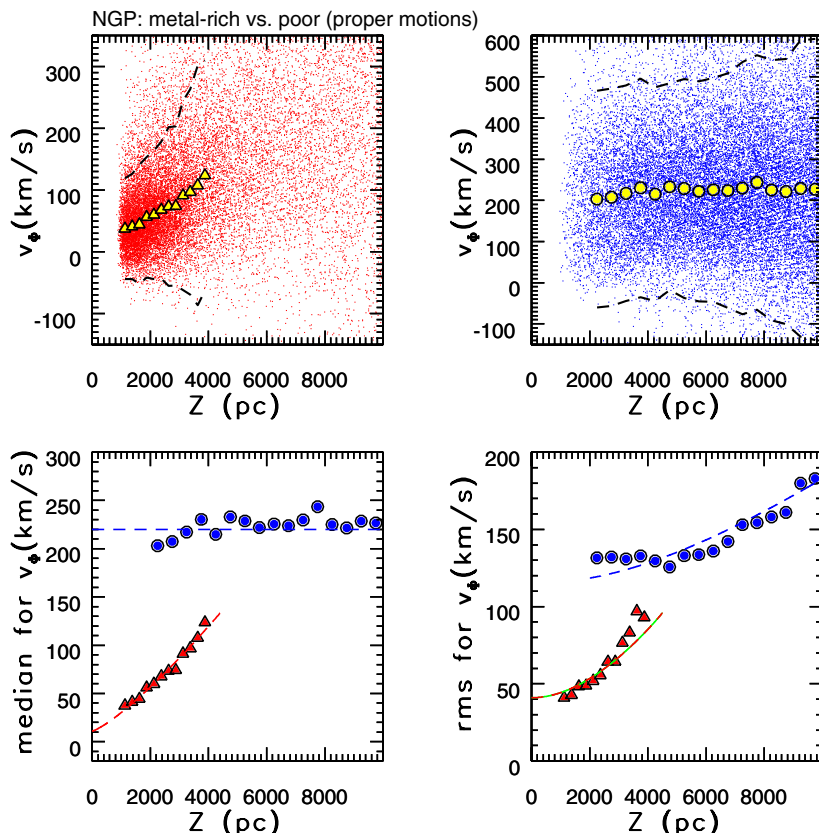


**Figure 1.** A comparison of the dependence of the rotational velocity component ( $v_{\Phi}$ , relative to the Sun, towards  $l = 270$ ) on distance from the galactic plane ( $Z$ ) for  $\sim 21,000$  high-metallicity (top left) and  $\sim 43,000$  low-metallicity (top right) F/G stars. In the top two panels, the small dots show individual stars, and the large symbols show the medians for  $Z$  bins. The dashed lines show the  $2\sigma$  envelope around these medians. The bottom two panels compare the medians (left) and velocity dispersions (right) for the two subsamples. The slightly curved dashed line in the bottom left panel describes velocity shear for disk stars:  $v_{\Phi} = (11 + 19.2(Z/\text{kpc})^{1.25})$  km/s. The dashed lines in the bottom right panel are predictions for the velocity dispersion based on known proper motion errors and an assumption of constant intrinsic dispersions (41 km/s for disk and 115 km/s for halo stars).

separated into 43,000 low-metallicity stars ( $[Fe/H] < -1$ , approximately  $u - g < 1$ ), and 21,000 high-metallicity stars. We use photometric metallicity estimates from Ivezić *et al.* (2008). The remaining 260,000 main-sequence stars with GKM spectral types, selected by  $g - r > 0.4$ , represent the third subsample. For all three subsamples, we estimate distance using the “bright” photometric parallax relation from Jurić *et al.* (2008). These distances have random errors of  $\sim 10\%$ , with comparable systematic errors for stars with the same metallicity.

The kinematic behavior of high-metallicity and low-metallicity F/G stars is remarkably different, as illustrated in Fig. 1. While this difference has been known since the seminal paper by Eggen, Lynden-Bell & Sandage (1962), here it is extended far from the solar neighborhood with  $\sim 100$  times larger samples. The disk stars display a strong non-linear velocity shear that can be reproduced with all color-selected subsamples. Although such subsamples can have vastly different apparent magnitudes and colors (and thus may be susceptible to different measurement errors), they all produce consistent results for

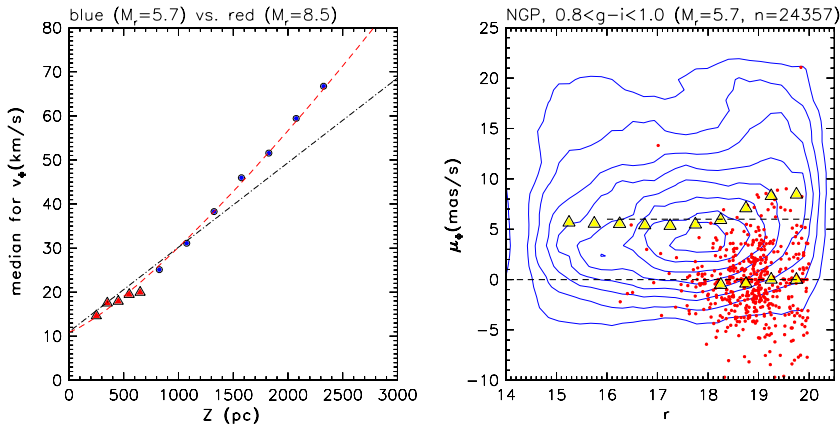


**Figure 2.** The left panel shows the dependence of the rotational velocity component on distance from the galactic plane for two color-selected samples of disk stars whose  $M_r$  differ by  $\sim 3$  mag. The two lines show  $v_\phi = (11 + 19.2(Z/\text{kpc})^k)$  km/s, for  $k = 1.0$  (lower, dot-dashed) and  $k = 1.25$  (upper, dashed). The right panel shows the rotational proper motion component as a function of apparent magnitude for the bluer sample as contours, with the medians shown by the upper set of large symbols. The non-linearity of the  $v_\phi$  vs.  $Z$  dependence shown in the left panel is seen here as an upturn of median proper motion for  $r > 18$ . This upturn is robust, as demonstrated by the quasar sample (dots) whose medians are consistent with zero (the lower set of large symbols).

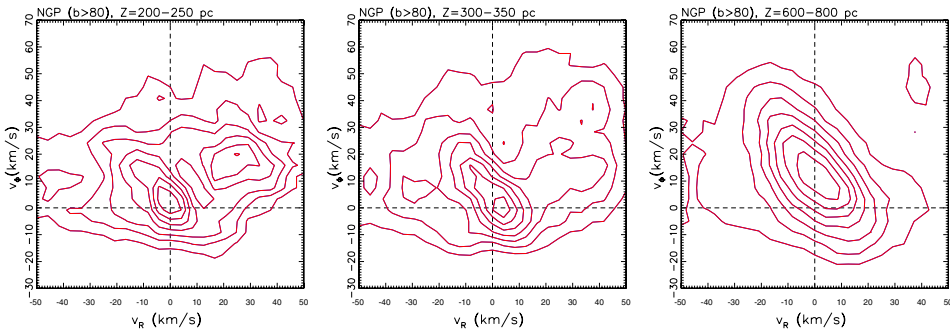


**Figure 3.** The velocity distribution for GKM dwarfs towards the north galactic pole for three narrow ranges of the distance from the galactic plane ( $Z$ , with 3600, 5600 and 29000 stars), as indicated on top of each panel. Note the significant changes of the distribution as  $Z$  increases.

the velocity shear, as illustrated in Fig. 2. As the color selection is extended to the more numerous and nearby M dwarfs, the velocity distribution function in the 0.1–1 kpc range can be studied in great detail, as illustrated in Fig. 3. Very close to the plane, the distribution resembles the rich structure seen in the solar neighborhood using Hipparcos data (Dehnen 1998), but we detect significant variation with  $Z$ .

### 3. The proper motion and parallax accuracy expected from LSST

The revolutionary progress in studies of the Milky Way kinematics enabled by the SDSS-POSS proper motion database will be maintained by the upcoming next-generation surveys, such as Pan-STARRS (Kaiser 2002) and LSST (Tyson 2002). The expected performance by Pan-STARRS is described by E. Magnier in these Proceedings. Here we focus on estimating the accuracy of proper motion and parallax measurements based on anticipated LSST astrometric data.

### 3.1. An overview of LSST

The LSST is currently the most ambitious proposed ground-based optical survey. The main science themes that drive the LSST system design are

- (a) Constraining Dark Energy and Dark Matter
- (b) Taking an Inventory of the Solar System
- (c) Exploring the Transient Optical Sky
- (d) Mapping the Milky Way

Driven by these science themes, the LSST will be a large, wide-field ground based telescope designed to obtain sequential images covering the entire visible sky from Cerro Pachon in Chile. The current baseline design (details are available at <http://www.lsst.org>), with an 8.4m (6.5m effective) primary mirror and a 9.6 sq.deg. field of view, will allow about 15,000 sq.deg. of sky to be covered in two photometric bands every three nights (assuming two 15-second exposures per field). The system is designed to yield high image quality as well as superb astrometric and photometric accuracy. The survey area will include 30,000 sq.deg. south from  $\delta = +34.5^\circ$ , and will be imaged multiple times in six bands covering the wavelength range 0.32–1.05  $\mu\text{m}$  (SDSS-like *ugriz* bands and the *y* band centered on 1  $\mu\text{m}$ ). The vast majority (about 90%) of the observing time will be devoted to a deep-wide-fast survey mode which will observe a 20,000 sq.deg. region close to 1000 times (including all bands) during the 10-year survey. The deep-wide-fast survey data will serve the majority of science programs. The remaining 10% of observing time will be allocated to special programs such as Very Deep and Very Fast time domain surveys.

### 3.2. Estimates of the proper motion and parallax accuracy

To estimate the proper motion and parallax accuracy, we use a sophisticated Operations Simulator which creates detailed realizations of the survey sky coverage and depth. The Simulator contains detailed models of site conditions, hardware and software performance, and an algorithm for scheduling observations which will, eventually, drive the robotic observatory.

Observing conditions include a model for seeing derived from an extensive body of on-site MASS/DIMM measurements obtained during site selection and characterization. Weather data are taken from ten years of nightly measurements at nearby Cerro Tololo. The signal to noise ratio of each observation is determined using a sky background model which includes the dark sky brightness in each filter, the effects of seeing and atmospheric transparency, and a model for scattered light from the moon and/or twilight at each observation. The time taken to move from one observation to the next is given by a detailed model of the camera, telescope, and dome. It includes such effects as the acceleration/deceleration profiles employed in moving in altitude, azimuth, camera rotator, dome azimuth, and wind/stray light screen altitude, the time taken to damp vibrations excited by each slew, cable wrap, and time taken for active optics lock and correction as a function of slew distance, filter change, and focal plane readout.

The result of a simulator run is a detailed history over a many-year period of which locations on the sky were observed when, in what filter, and with what sky background, seeing and other observing conditions. The median expected number of visits (two 15-second back-to-back exposures) for the baseline main survey ( $\sim 20,000$  sq.deg.) is listed in Table 1.

Given the observing sequence for each sky position in the main survey, we generate a time sequence of mock astrometric measurements. The assumed astrometric accuracy is a function of signal-to-noise,  $SNR$ . Random astrometric errors are modeled as  $\theta/SNR$ , with  $\theta = 700$  mas. The estimated proper motion and parallax accuracy at the bright end

Filter	u	g	r	i	z	y
Single visit depths ( $5\sigma$ )	23.9	25.0	24.7	24.0	23.3	22.1
Mean number of visits	56	80	184	184	160	160
Final (coadded) depths ( $5\sigma$ )	26.2	27.4	27.6	26.9	26.1	24.8

**Table 1.** The expected median  $5\sigma$  depths for point sources per single visit (two 15-second exposures), the median number of visits over a 10-year long LSST baseline survey, and expected depths when all observations are co-added.

( $r < 20$ , note that  $V \sim r$ ) is driven by systematic errors. Systematic errors of 10 mas are added in quadrature, and are assumed to be *uncorrelated* between different observations. Systematic and random errors become similar at about  $r = 22$ , and there are about 100 stars per LSST CCD (0.05 sq. deg) to this depth (and fainter than LSST saturation limit) even at the galactic poles.

Pre-cursor data from the Subaru telescope indicate that systematic errors of 10 mas are not too optimistic. Even a drift-scanning survey such as SDSS delivers uncorrelated systematic errors (dominated by seeing effects) at the level 20-30 mas (measured from repeated scans), and the expected image quality for LSST will be twice as good as for SDSS. Furthermore, there are about 1000 galaxies per CCD with  $r < 22$ , which will provide exquisite control of systematic astrometric errors as a function of magnitude, color and other parameters.

The astrometric transformations for a given CCD and exposure, and proper motion and parallax for all the stars from a given CCD, are simultaneously solved for using an iterative algorithm. The astrometric transformations from pixel to sky coordinates are modeled using low-order polynomials and standard techniques developed at the US Naval Observatory. The expected proper motion and parallax errors for a 10-year long baseline survey, as a function of apparent magnitude, are summarized in Table 2. Blue stars (e.g. F/G) fainter than  $r \sim 23$  will have about 50% larger proper motion and parallax errors due to decreased number of the  $z$  and  $y$  band detections. The impact on red stars is smaller due to relatively small number of observations in the  $u$  and  $g$  bands, but extremely red objects, such as L and T dwarfs, will definitely have larger errors, depending on details of their spectral energy distribution. As a function of time, the proper motion errors are about five times as large, and parallax errors are about twice as large after the first three years of the survey.

$r$ mag	$\sigma_{xy}^a$ mas	$\sigma_\pi^b$ mas	$\sigma_\mu^c$ mas/yr	$\sigma_1^d$ mag	$\sigma_C^e$ mag
21	11	0.6	0.2	0.01	0.005
22	15	0.8	0.3	0.02	0.005
23	31	1.3	0.5	0.04	0.006
24	74	2.9	1.0	0.10	0.009

*Notes:*

<sup>a</sup> Typical astrometric accuracy (per coordinate); <sup>b</sup> Parallax accuracy; <sup>c</sup> Proper motion accuracy; <sup>d</sup> Photometric error for a single visit (two 15-second exposures); <sup>e</sup> Photometric error for coadded observations (see Table 1)

**Table 2.** The expected proper motion, parallax and photometric accuracy, as a function of apparent magnitude  $r$ , for a 10-year long LSST baseline survey. For comparison, the SDSS-POSS proper motion measurements have an accuracy of  $\sim 5$  mas/yr per coordinate at  $r = 20$ . Gaia is expected to deliver parallax errors of 0.3 mas, and proper motion errors of 0.2 mas/yr at its faint end at  $r \sim 20$ . LSST will smoothly extend Gaia's error vs. magnitude curve to a 4 magnitude fainter level.

#### 4. Discussion and conclusions

The SDSS-POSS proper motion database developed by Munn *et al.* (2004) is a powerful tool to study the Milky Way kinematics. The accuracy of  $\sim 3$  mas/yr for tens of millions of stars with  $r < 20$  is not only a quantitative, but also a major qualitative step forward. This accuracy to such a depth enables the extension of kinematic studies beyond the solar neighborhood, and the availability of a large number of stars (essentially a complete flux-limited sample in a given region of the sky) offers an unprecedented spatial resolution. We presented here only a small selection of kinematic results that are based on this dataset, and discussed in detail by Bond *et al.* (2008). These results vividly demonstrate the power of massive and accurate proper motion measurements to faint flux levels for understanding kinematics, dynamics and the assembly history of the Galaxy.

As suggested by its expected proper motion and parallax accuracy listed in Table 2, LSST will enable major breakthroughs in the mapping of stellar motions by delivering the Hipparcos accuracy to the SDSS depth for hundreds of millions of stars. For example, numerous main sequence F/G stars with  $0.2 < g-r < 0.4$  have  $M_r \sim 4$ . LSST will detect about 100 million such stars with  $r < 22$  (Ivezić *et al.* 2008). At  $r = 22$ , they probe the outer halo at distances of  $\sim 40$  kpc, and LSST will measure their tangential velocity with errors as small as  $\sim 50$  km/s. Neither SDSS-POSS proper motions, nor expected Gaia data, can be used to perform such massive and accurate kinematic measurements in the outer halo. At the red end of the main sequence, M dwarfs with  $M_r = 12$  (i.e. the peak of the main-sequence luminosity function) will have tangential velocity errors of 1 km/s at 1 kpc ( $r = 22$ ), and 12 km/s at 2.5 kpc ( $r = 24$ ). For sub-stellar objects with  $r = 22$ , geometric parallax measurements will yield 10% accurate distances for *all* objects brighter than  $M_r = 17$  within a 100 pc half-sphere. We estimate that this sample will include about 10,000 objects with  $16 < M_r < 17$  ( $r < 22$ ), that will provide unprecedentedly robust and accurate measurement of the stellar luminosity function at its faint end.

LSST and Gaia will be highly complementary surveys. Gaia will obtain much more accurate measurements for  $r < 20$ , but LSST will extend them 4 magnitudes deeper. Thanks to the 3-4 magnitudes of overlap between the surveys, Gaia's parallax measurements will be used to train photometric parallax estimators as a function of effective temperature and metallicity, and perhaps gravity, and Gaia's proper motion measurements will be used to verify the accuracy of measurements by LSST.

Ž.I. and B.S. acknowledge support by NSF grants AST-0551161 and AST-0707901.

#### References

- Adelman-McCarthy, J. K., Agüeros, M. A., Allam, S. S., *et al.* 2006, ApJS, 162, 38  
 Dehnen, W. 1998, AJ, 115, 2384  
 Dehnen, W. & Binney, J. J. 1998, MNRAS, 298, 387  
 Eggen, O. J., Lynden-Bell, D., & Sandage, A. R. 1962, ApJ, 136, 748  
 Ivezić, Ž., Tabachnik, S., Rafikov, R., *et al.* 2001, AJ, 122, 2749  
 Ivezić, Ž., Sesar, B., Jurić, M., *et al.* 2008, submitted to ApJ  
 Jurić, M., Ivezić, Ž., Brooks, A., *et al.* 2008, ApJ, in press  
 Kaiser, N., Aussel, It., Burke, B. E., *et al.* 2002, in "Survey and Other Telescope Technologies and Discoveries", Tyson, J. A. & Wolff, S., eds. Proceedings of the SPIE, 4836, 154  
 Munn, J. A., Monet, D. G., Levine, S. E., *et al.* 2004, AJ, 127, 3034  
 Pier, J. R., Munn, J. A., Hindsley, R. B., *et al.* 2003, AJ, 125, 1559  
 Pourbaix, D., Knapp, G. R., Szkody, P., *et al.* 2005, A&A, 444, 643  
 Schneider, D. P., Hall, P. B., Richards, G. T. *et al.* 2007, AJ, 134, 102  
 Tyson, J. A. 2002, in *Survey and Other Telescope Technologies and Discoveries*, Tyson, J. A. & Wolff, S., eds. Proceedings of the SPIE, 4836, 10